Cation Ordering in Synthetic Layered Double Hydroxides

Article *in* Clays and Clay Minerals · December 1997

DOI: 10.1346/CCMN.1997.0450604

3 authors, including:

Geoff D. Moggridge
University of Cambridge
125 PUBLICATIONS **2,280** CITATIONS

Clays and Clay Minerals, Vol. 45, No. 6, 803–813, 1997.

CATION ORDERING IN SYNTHETIC LAYERED DOUBLE HYDROXIDES

M. VUCELIC,[1] W. JONES[1] AND G. D. MOGGRIDGE[2]

[1] Chemistry Department, University of Cambridge, Lensfield Rd., Cambridge CB2 1EW, United Kingdom

[2] Chemical Engineering Department, University of Cambridge, Pembroke St., Cambridge CB2 3RA, United Kingdom

Abstract—A combined powder X-ray diffraction (XRD) and X-ray absorption (XAS) study of Fe(III) cation ordering within pyroaurite is described. It is concluded that there is no correlation between Fe(III) cation positions over distances of a few tens of angstroms, but that there is a very high level of local ordering, involving the absence of Fe(III)-Fe(III) neighbors. These observations are rationalized in terms of a significant frequency of lattice defects in the form of cation vacancies or Mg for Fe(III) substitutions. These results are expected to be generalizable to other M(II)/M(III) layered double hydroxides (LDHs), but are in contrast to the long-range cation ordering observed in Li/Al LDHs. This raises the interesting possibility of differing properties and stabilities based on the degree of cation ordering.

Key Words—Cation Ordering, LDH, Pyroaurite, XAS, XRD.

INTRODUCTION

One class of anionic layered minerals is the LDHs (Frondel 1941; Allmann 1968, 1970; Taylor 1969, 1973; Serna et al. 1982), having the general formula:

$$\{M_{1-x}^{II}M_x^{III}(OH^-)_2\}^{x+}\ (A^{m-})_{x/m}\cdot nH_2O$$

The commonest types of LDH are the hydrotalcite group of minerals (Gastuche et al. 1967; De Waal and Viljoen 1971; Miyata 1975; Brindley and Kikkawa 1979; Drezdon 1988), in which the cations are Mg and Al, and the pyroaurites, in which the cations are Mg and Fe(III) (Ulibarri et al. 1987; Hansen and Taylor 1990, 1991). These grow as very small, hexagonal crystals, the structure being derived from that of brucite. Each cation is octahedrally surrounded by hydroxides, the octahedra sharing edges to form 2-dimensional sheets. These sheets carry an excess positive charge due to the presence of the triply charged cations and this is balanced by interlayer anions that bind the sheets together. It is possible to substitute a wide variety of inorganic or organic anions into the interlayer, either by ion exchange or synthetically (Miyata 1975; Drezdon 1988; Chibwe and Jones 1989; Borja and Dutta 1992) and this has resulted in substantial academic and industrial interest in this type of mineral (Reichle 1985; Kuma et al. 1989; Jones 1991).

It is well established (Allmann 1968, 1970) that the structure of the 2-dimensional hydroxide sheets in LDHs is very close to that of brucite; however, the relative positions of the 2 types of cations present is poorly understood. It has long been speculated that there is cation ordering within the 2-dimensional sheets (Gastuche et al. 1967; Taylor 1969, 1973; Allmann 1970; Brindley and Kikkawa 1979). In particular, it is often argued that triply positive cations will never occupy neighboring cation sites; credence is given to this idea by the fact that III:II cation ratios do not seem to exceed 1:2 in either naturally occurring or synthetic minerals (Pausch et al. 1986 have recently reported synthetic hydrotalcites with a III:II ratio of more than 1:2, but only following extreme synthetic conditions). If triply charged cations cannot be neighbors, then this ratio should result in a completely ordered superlattice with unit-cell parameters in the brucite-like sheets of $\sqrt{3}a$ (a being the mean cation–cation distance) and the hexagonal lattice rotated by 30° from that of brucite. Materials with a whole range of cation ratios down to 1:6 may be synthesized and other patterns of cation ordering have been suggested for these.

In this paper we report on a powder XRD and XAS study of Fe(III) cation ordering in pyroaurites. Diffraction probes the long-range order (tens of angstroms and more) in crystalline materials and thus allows one to establish whether there is a highly ordered 2-dimensional superlattice present. Such superlattices have been observed by powder XRD previously in the Li/Al LDHs, in which the Li ions fill vacancies in a gibbsite-like structure and so naturally form a long-range superlattice (Serna et al. 1982; Sissoko et al. 1985; Dutta and Puri 1988), and as a result of anion ordering of sulphate (Bookin et al. 1993) or benzoate (Vucelic et al. 1995) in the interlayer of hydrotalcites, where geometric factors force a high degree of ordering into the interlayer region. By contrast, XAS probes the local structure around an absorbing atom and so allows observation of short-range ordering (up to about 6–8 Å) in crystalline or amorphous materials; thus it is ideal when looking for effects such as triply charged cations not sitting in neighboring sites within brucite-like layers.

So these 2 techniques are complementary and provide powerful means for assessing the degree of cation ordering in LDHs. Although if either the local or long-range order described above is perfect, it must result in the other type also being present, often imperfec-

tions can result in only 1 type being detectable. For example, short-range order is excellent in glasses, but no crystalline structure is observable, while in the case of the anion ordering within the LDHs described above there are certainly many deviations from the ideal local site but, on average over a long distance, the electron density oscillates regularly.

We have chosen to study pyroaurite, that is, LDHs with Fe(III) and Mg as cations. Reasons for studying this material are that it is common and widely used and because Fe and Mg are widely separated in the periodic table. The large difference in the number of electrons in the 2 cations means that they have very different X-ray scattering powers and so show good contrast in XRD; thus, Fe superlattices should result in strong diffraction features. Similarly, the electron scattering cross section and the phase shift of backscattered electrons is very different for Fe and Mg and so the 2 cations should be easily distinguished in extended X-ray absorption fine structure (EXAFS) studies; hence local ordering should also be detected without difficulty. Three pyroaurites with Fe:Mg ratios of approximately 1:2, 1:3 and 1:4 were used to determine the effect of Fe concentration on Fe(III) cation ordering, as has been speculated in the literature (see for example Brindley and Kikkawa 1979). In all cases described below carbonate was used as counterion; carbonate seems to be the most stable interlayer anion, resulting in the highest degree of crystallinity and lowest levels of contaminants in synthetic LDHs and so should give the best opportunity for observing cation ordering. However, the results should be applicable to other interlayer anions. To check this, a 1:2 Fe:Mg pyroaurite with interlayer benzoate was also investigated by XAS; the results were indistinguishable from those for the carbonate pyroaurite (for brevity this material will not be described further).

EXPERIMENTAL

The LDHs were prepared by direct synthesis. A stoichiometric mixture of $Mg(NO_3)_2$ and $Fe(NO_3)_3$ was dribbled into excess sodium carbonate dissolved in sodium hydroxide solution, over a period of about 1 h with vigorous stirring at room temperature; the final pH was approximately 11. The resulting amorphous slurry was then heated at 75 °C for 18 h with vigorous stirring, to allow crystallization. The crystals were filtered, washed to neutrality and dried at about 50 °C.

It has been shown (Gastuche et al. 1967; Brindley and Kikkawa 1979; Miyata 1980) that under these conditions of LDH synthesis, the II:III cation ratio in the solution is reflected in the solid LDH formed over a wide range of compositions. This can be checked by observation of the *a* lattice parameter, which decreases linearly with increasing trivalent cation composition.

The Fe:Mg ratios of the samples synthesized were checked by elemental analysis using energy dispersive fluorescence analysis. The measured Fe:Mg ratios were 1:2.17, 1:2.98 and 1:3.79. It is interesting to note that although close to the nominal values of 1:2, 1:3 and 1:4, respectively, the cation ratios always tend towards 1:3. This is consistent with the observation that natural LDH minerals predominantly have a 1:3 III:II cation ratio and the authors' hypothesis that longer and fiercer synthetic conditions drive hydrotalcites towards a 1:3 Al:Mg ratio (Vucelic et al. 1995).

Powder diffraction patterns were collected using a Philips PW1710 diffractometer with a Cu anode and 1° divergence slits, using 0.04° step size.

X-ray absorption data were recorded at the Fe *K*-edge in transmission geometry on the EXAFS 3 beamline at the high-energy synchotron ring (DCI), Laboratoire pour l'Utilisation du Rayonnement Electromagnetique (LURE) and on station 8.1 at Daresbury in Chesire, United Kingdom; in both cases a Si[220] double crystal monochromator was used. Harmonic rejection was set at 50%. Absorption was detected using He/Ar filled ion chambers (currents were of the order of 10^{-7} mA for I_0 and 10^{-8} mA for I_t). Samples were prepared by thoroughly grinding sufficient sample to give an edge step of about 1 with boron nitride and then pressing into 13-mm-diameter discs.

Background subtraction was achieved using the EXBACK program; the pre-edge was taken as linear and a single third-order polynomial was used for the post edge. E_0 was taken as the point halfway up the edge step. EXCURVE92 was used for data analysis; this program was also used to calculate theoretical phase shifts. These phase shifts were checked using a standard α-Fe_2O_3 sample (Aldrich—checked for phase purity by powder XRD) (see Figure 2 and Table 2). Models were refined using a least-squares fitting procedure.

RESULTS

Figure 1 is a stack plot of the powder XRD patterns for the 3 pyroaurite samples with Fe:Mg ratios of 1:2, 1:3 and 1:4. All the peaks present in each of the 3 patterns can be assigned on the basis of a hexagonal cell with *a* being the shortest cation–cation distance and *c* 3 layer spacings (see Table 1). The 3-layer unit-cell distance and the systematic absence of reflections other than $-h + k + l = 3n$ demonstrate that all 3 materials have rhombohedral symmetry, the complete dominance of 01*l* reflections over 10*l*s strongly suggesting that the structure is AC = CB = BA = AC (following the notation of Bookin and Drits 1993). As the Fe loading increases, a slight decrease in the 110 *d*-spacing is observed. This is consistent with increasing amounts of trivalent cation in the brucite-like layers, since the more positive ions are expected to attract the hydroxides more strongly and so reduce the average *a* lattice parameter ($a = 2d_{110}$). Indeed a linear relationship between trivalent cation loading and d_{110} for LDHs (Brindley and Kikkawa 1979) has been re-

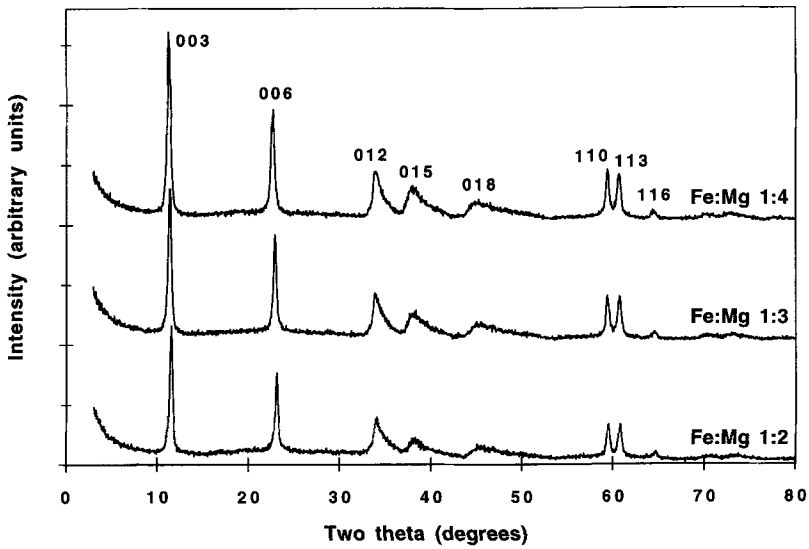

Figure 1. Powder XRD patterns of synthetic pyroaurites with different Fe:Mg ratios. (Patterns are offset vertically for clarity.)

ported and the values of Table 1 are fully consistent with the nominal Fe loadings of the LDHs. Similarly the *d*-spacings of the 00*l* reflections can be seen to reduce slightly as the Fe loading increases. Again this can be attributed to the higher charges (this time the net charge on the layers and therefore in the interlayer spaces) pulling the structure together more strongly.

Apart from these minor differences in lattice parameters and small variations in peak intensities (which can be attributed to the differing scattering powers of Mg and Fe and possibly some variation in the static disorder present in the 3 compounds), the 3 patterns are identical. This very great similarity in all the patterns immediately suggests that there is no long-range Fe(III) cation ordering (that is, ordering on a length scale beyond a few tens of angstroms), since if there were any the unit cell size and shape would have to change as the Fe loading varied. This is confirmed by the fact that all peaks can be assigned using a unit cell based on the shortest cation–cation distance; that is, all regular fluctuations in the electron density within the brucite-like layer occur with a period of less than the distance between neighboring cations, precluding the possibility of there being any kind of superlattice present. In LDH systems where superlattices have been observed (Li-Al hydroxides and hydrotalcites with sulphate and benzoate as anions), reflections are always seen at around 19–20 °2θ, corresponding to the 100 superlattice reflection (Bookin et al. 1993; Vucelic et al. 1995). In our case, for the 1:2 Fe:Mg pyroaurite, one expects a superlattice with unit cell of $\sqrt{3}a$, corresponding to a reflection at about 19.0 °2θ (d = 4.67 Å), if Fe cations never neighbor each other. No such reflection is observed and the diffraction pattern is completely flat in this region; the superlattice feature cannot be hidden beneath another reflection. In the case of the lower Fe loading pyroaurites, even larger superlattice parameters would be expected; again these should result in obvious features in the diffraction pattern, which are clearly absent. Thus the diffraction results unambiguously demonstrate that over a few tens of angstroms, Fe(III) cation ordering is completely absent over the whole range of Fe loadings. Over this type of distance the distribution of divalent and trivalent cations is completely statistical and it will be impossible to predict the position of 1 iron atom from that of another.

Table 1. Summary of powder XRD patterns of pyroaurites with various Fe:Mg ratios.

	Peak position (*d*-spacing/Å)		
Assignment	Fe:Mg 1:2	Fe:Mg 1:3	Fe:Mg 1:4
003	7.68	7.74	7.83
006	3.85	3.87	3.91
012	2.63	2.65	2.65
015	2.36	2.37	2.37
018	1.99	2.00	2.02
110	1.55	1.56	1.56
113	1.52	1.52	1.53
116	1.44	1.44	1.44
119	1.33	1.33	1.34
0018	1.29	1.29	1.30

X-ray absorption studies were carried out to establish the extent of local Fe(III) cation ordering. Analysis of the fine structure beyond the edge in XAS depends on the interference of backscattered electron waves with the outgoing photo-ejected electron. Due to the short mean free path of electrons in a solid, information can only be obtained to a distance of several angstroms from the absorbing atom. Thus, in the

Table 2. Comparison of crystallographic data (structure reference 6044, inorganic crystal structure database (ICSD), Daresbury Laboratory) and best-fit XAS parameters for Fe_2O_3 standard. Raw data Fourier-filtered beyond 4.1 Å to remove higher shell contributions. Note the absence of light scatterers from the fitted fine structure beyond 2.5 Å.

Crystallographic data			Best-fit parameters			
Atom type	Number of atoms	Distance (Å)	Atom type	Number of atoms	Distance (Å)	Debye–Waller factor (Å²)
O	3	1.946	O	3	1.94	0.023
O	3	2.116	O	3	2.11	0.025
Fe	1	2.900	Fe	1	2.91	0.009
Fe	3	2.971	Fe	3	2.98	0.011
Fe	3	3.364	Fe	3	3.38	0.012
O	3	3.399	—	—	—	—
O	3	3.596	—	—	—	—
Fe	6	3.705	Fe	6	3.71	0.012
O	3	3.786	—	—	—	—
Fe	1	3.986	Fe	1	3.98	0.007
			E_0 (eV)	VPI (Å)	AFAC	R-factor
			0.00	−4.00	0.88	7.68

case of pyroaurite, one can only expect to be able to interpret features arising from (see Figures 3, 4 and 5) the first hydroxide shell (at 2.06 Å) and the first cation shell (3.11 Å) around the absorbing Fe. Due to their significantly different atomic numbers, it should be a relatively simple matter to distinguish Fe from Mg in this first cation shell. Generally one expects more backscattering from heavier elements and so Fe should show up more strongly in EXAFS than Mg; hence the intensity of the second shell (first cation shell) in the pseudo-radial distribution function (PRDF) would be expected to drop as the Fe loading drops if the cations were completely randomly distributed. Inspection of Figures 3, 4 and 5 and Table 3 show that this is clearly not the case and so one is led to suspect at least some degree of Fe(III) cation ordering. If the cations are perfectly ordered on a local level, there should never be any Fe neighboring another Fe and so all the cations in the 3.11-Å shell should be Mg, regardless of the Fe loading, and to first approximation one expects the EXAFS and PRDFs of the 3 pyroaurites to be the same. This can be seen to be roughly true simply by inspecting Figures 3, 4 and 5.

To be more quantitative about the results it is necessary to model the EXAFS obtained. For this to be possible one needs to establish the phase shifts caused to the backscattered electrons by each atom type present over the full range of photo-electron energies used. This was done by calculation using EXCURV92. To test the validity of the results, the phase shifts were used to model a standard compound, α-Fe_2O_3, of known structure (the structure was taken from the inorganic structure data base at Daresbury). The results are shown in Table 2 and Figure 2. Figure 2 shows k^3-$\chi(k)$ and the PRDF obtained by Fourier transforming this into r-space. The data have been Fourier-filtered in the range 0–4.1 Å; this was necessary before fitting because in the raw data there were significant oscillations resulting from shells at greater distances, but in the real structure there are so many different shells beyond 4 Å that any attempt at analysis could not be statistically significant. Oxygen backscattering from atoms at a distance greater than 3 Å was found to be too weak to be detectable and so the data could be fit by 7 shells as shown in Table 2. The data were fitted by fixing the coordination numbers at their crystallographic values and then optimizing the distances and Debye–Waller factors along with E_0, VPI and amplitude factor (AFAC). Thus there were 17 free parameters, well within the statistically significant $2\Delta k\Delta R/\pi$ (Δk being about 14 and ΔR = 3). It can be seen that a very good fit is obtained and Table 2 shows that the distances obtained are extremely close to the crystallographic values expected. This confirms that the calculated phase shifts are acceptable, at least for O and Fe. No standard compound containing Fe and Mg was readily available, so the phase shifts for Mg have not been directly confirmed in this way. However the Fe-Mg first shell distance is accurately known from the powder XRD results and the values of E_0, VPI and AFAC are largely determined by the stronger scattering from the first oxygen shell in the pyroaurites; thus given that the oxygen phase shift is adequate, the pyroaurites themselves can be used as self-standardizing compounds for the Mg phase shifts. If the Mg phase shifts were not good, either a poor fit or a nonphysical Mg-Fe distance would result.

Figures 3, 4 and 5 show the $k^3-\chi(k)$ (3–14 Å^{-1}) and the PRDF extracted from the XAS for pyroaurites with Fe:Mg ratios of 1:2, 1:3 and 1:4, respectively, as well as the best fits obtained for each set of data. Since no significant EXAFS was obtained from backscatterers beyond 3.5 Å, it was not necessary to Fourier filter before modeling, and so the raw data are displayed. Best-fit models were obtained by setting the coordination numbers for the first (O) and

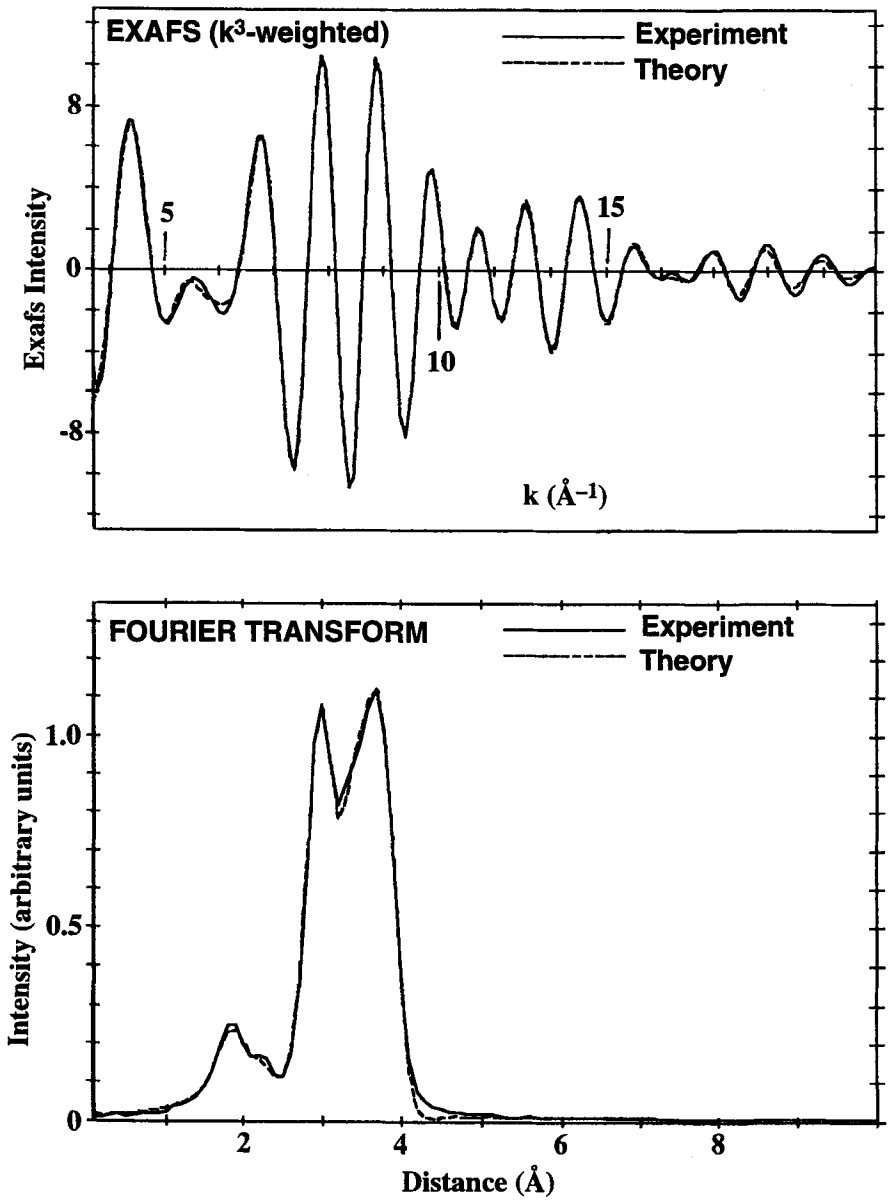

Figure 2. XAS fine structure (top) and its Fourier transform (bottom) for Fe_2O_3 (hematite). Data Fourier filtered beyond 4.1 Å and best-fit model based on cystallographic structure (ICSD, Daresbury Laboratory) shown.

second (Mg) shells to their "correct" values of 6 and optimizing the distances and Debye–Waller factors (along with E_0, VPI and AFAC) using a least-squares refinement. An alternative model was also tried to fit the data; the cation shell was fitted with the correct (assuming random distribution) fraction of Fe and Mg. The coordination numbers, bond lengths and Debye–Waller factors for both the Fe and Mg shells were then allowed to vary either freely or in a constrained manner. If the Fe-Fe distance was constrained to a physically reasonable value, the coordination number for the Fe always reduced to zero, while if the bond length and coordination number of the Fe were allowed to vary simultaneously (with or without the Mg shell parameters), either the Fe coordination number would reduce to zero or the bond length would become unphysical (and the coordination number reduce to a small or negative value). Thus, however the data were modeled, it was impossible to find evidence of the presence of any Fe at all in the cation shell neighboring the absorbing Fe atom. This was equally true for all 3 Fe:Mg ratio pyroaurites studied. This result demonstrates that there is a high degree of local Fe(III) cation ordering present

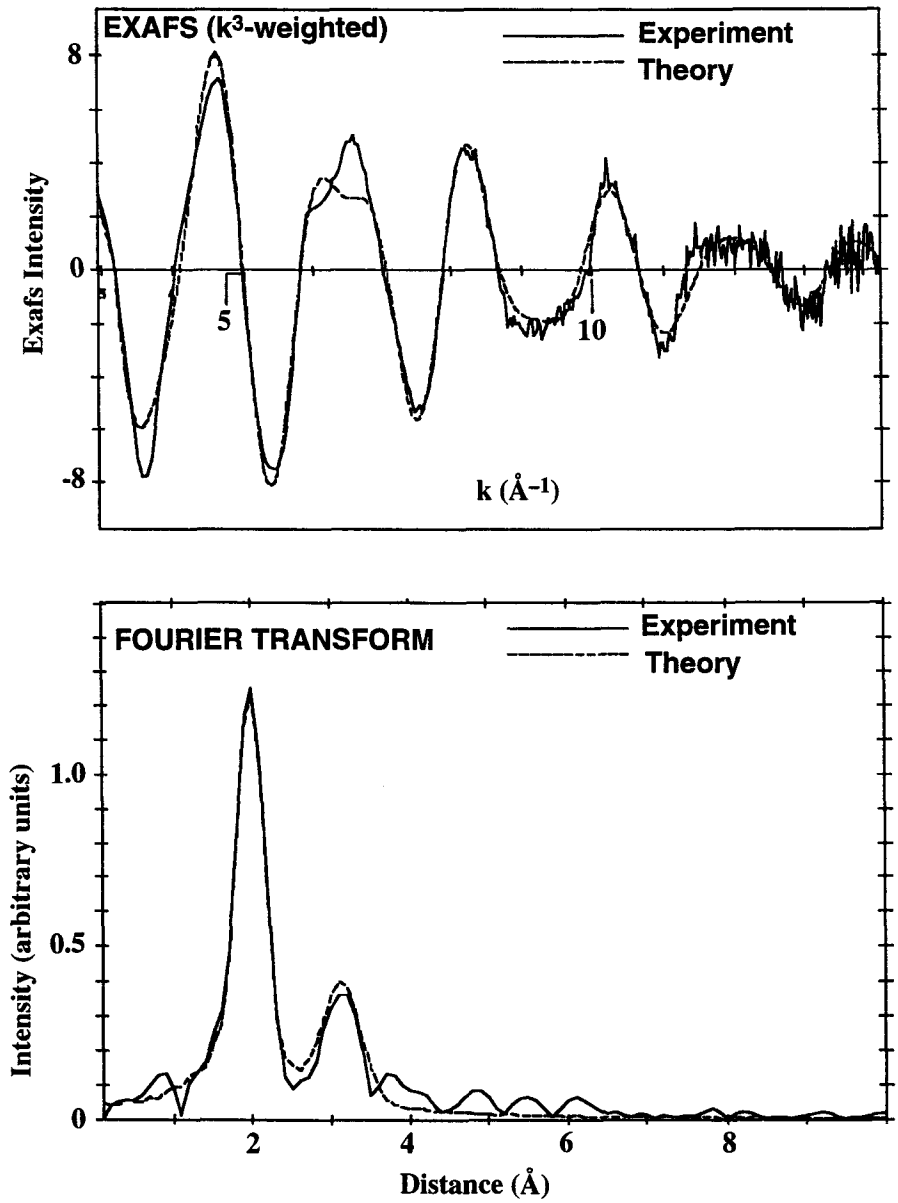

Figure 3. XAS fine structure (top) and its Fourier transform (bottom) for synthetic pyroaurite with Fe:Mg 1:2. Raw data and best-fit model (obtained by optimizing O, Mg and Fe shells) shown.

in pyroaurite, in the form of Fe cations avoiding each other as nearest neighbors.

Figure 6 is designed to show how easy it would be to detect Fe if it were present in the first cation shell. The data shown in both the top and bottom panels is $k^3-\chi(k)$ EXAFS of the Fourier-filtered (2.2–4 Å) second shell (cation shell) of the 1:2 Fe:Mg pyroaurite. In the top panel the fitted Mg shell (6 atoms at 3.11 Å) from the best fit of Figure 3 is also displayed; it is nicely in phase with and has an amplitude envelope which follows closely that of the data. In the bottom panel is shown model EXAFS data for an Fe shell of 2 atoms placed at the same distance (3.11 Å); it can be seen to be completely out of phase with and have a totally different amplitude envelope to the data. Thus it should be no problem to distinguish EXAFS resulting from Fe from that produced by Mg atoms at the same distance. Moreover it can be seen from Figure 6 that 2 Fe atoms produce roughly the same backscattering amplitude as 6 Mg (this is due to the greater number of electrons present in Fe). Therefore it should be possible to distinguish a relatively small Fe concentration in the first cation shell, certainly as low as 5%. This shows that the correlation between Fe cation

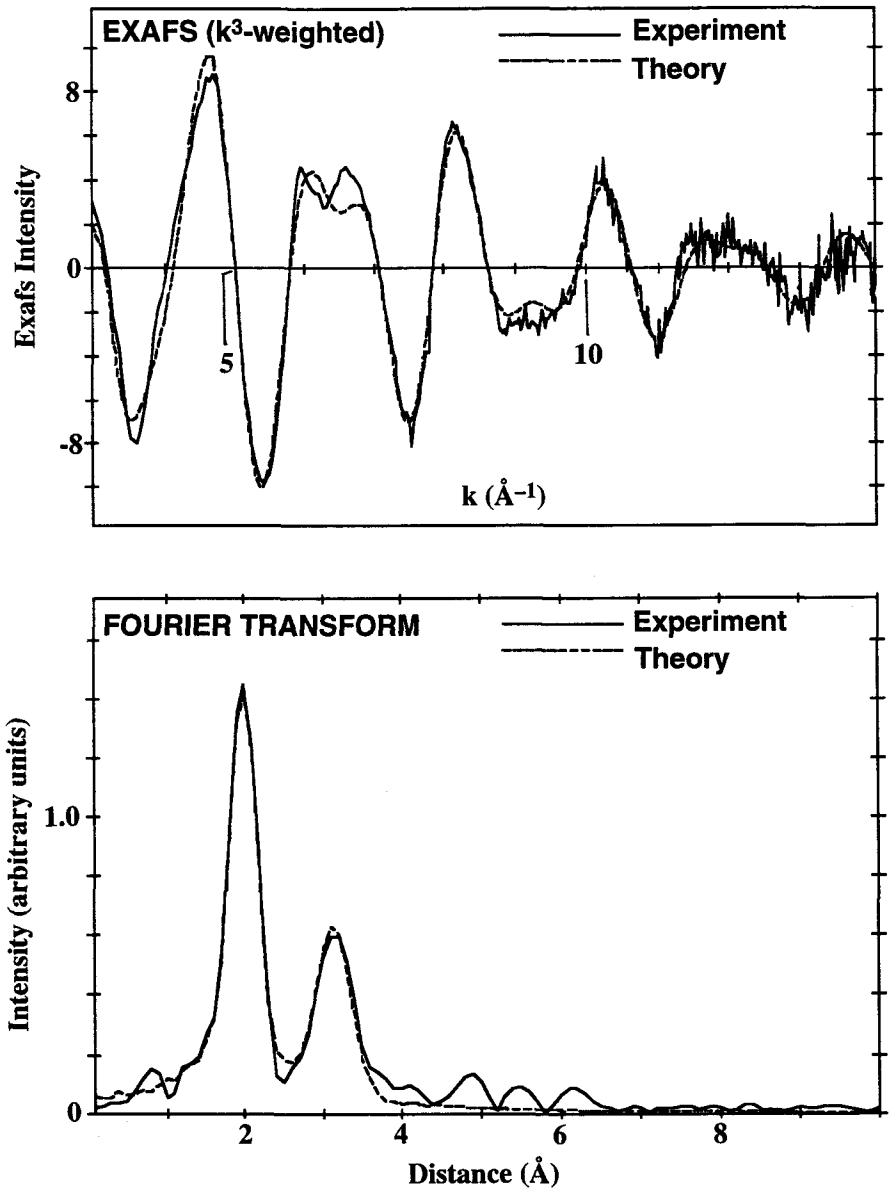

Figure 4. XAS fine structure (top) and its Fourier transform (bottom) for synthetic pyroaurite with Fe:Mg 1:3. Raw data and best-fit model (obtained by optimizing O, Mg and Fe shells) shown.

positions is very good over distances of a few angstroms—at most 1 in 20 cations neighboring Fe(III) also being Fe(III).

Table 3 contains the best-fit parameters for the 3 spectra and the values of coordination number and distance that would be expected on the basis of a perfect brucite-like lattice, the lattice parameters being obtained from the powder XRD data. As can be seen, the agreement is very good indeed. Not only do the XAS data provide absolutely no evidence for the presence of significant amounts of Fe in the first cation coordination sphere, but the data can also be satisfactorily explained on the basis of a model involving only 1 O and 1 Mg shell, with distances and coordination numbers in complete accord with the diffraction data.

The only significant difference between the best-fit parameters obtained for the 3 pyroaurites (other than the expected slight contraction of the lattice with increasing Fe loading) is in the Debye–Waller factor for the material with 1:2 Fe:Mg ratio. This is rather higher (0.018 Å^2) than for the other 2 pyroaurites (0.0012–0.0013 Å^2), indicating a rather greater degree of disorder in the lattice. This is consistent with the slightly smaller intensity of the 11*l* reflections in the diffraction pattern of the 1:2 Fe:Mg pyroaurite compared to the other two; this too could be caused by greater dis-

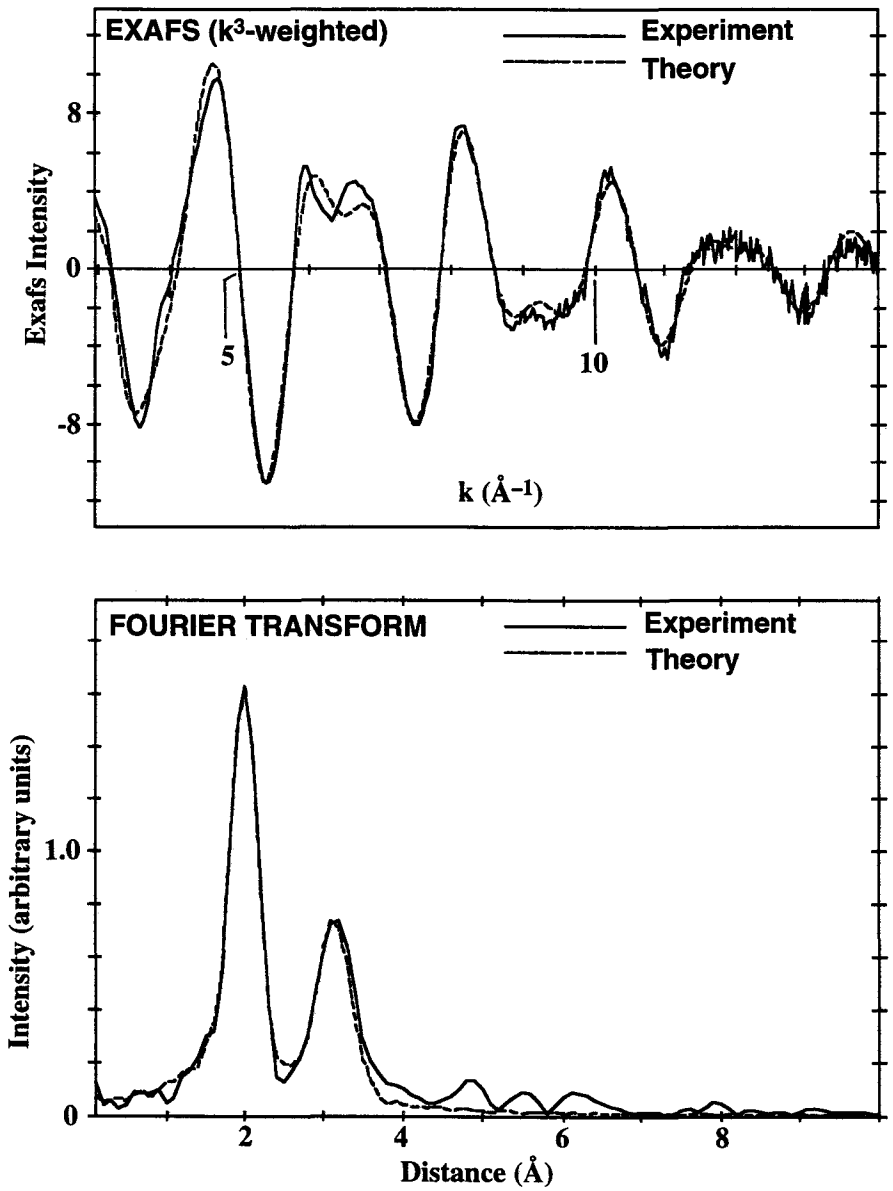

Figure 5. XAS fine structure (top) and its Fourier transform (bottom) for synthetic pyroaurite with Fe:Mg 1:4. Raw data and best-fit model (obtained by optimizing O, Mg and Fe shells) shown.

Table 3. Best-fit XAS parameters for pyroaurites with Fe:Mg ratios of 1:2, 1:3 and 1:4. Fits are to raw data.

		Fe:Mg 1:2 (Figure 3)	Fe:Mg 1:3 (Figure 4)	Fe:Mg 1:4 (Figure 5)
First shell (O)	Number of atoms	6	6	6
	Distance (Å)	2.00	2.01	2.01
	Debye–Waller factor (Å²)	0.010	0.011	0.010
Second shell (Mg)	Number of atoms	6	6	6
	Distance (Å)	3.11	3.12	3.12
	Debye–Waller factor (Å²)	0.018	0.013	0.012
	E_0 (eV)	0.00	0.00	0.00
	VPI (Å)	−4.00	−4.00	−4.00
	AFAC	0.68	0.81	0.87
	R-factor	24.6	24.3	19.9

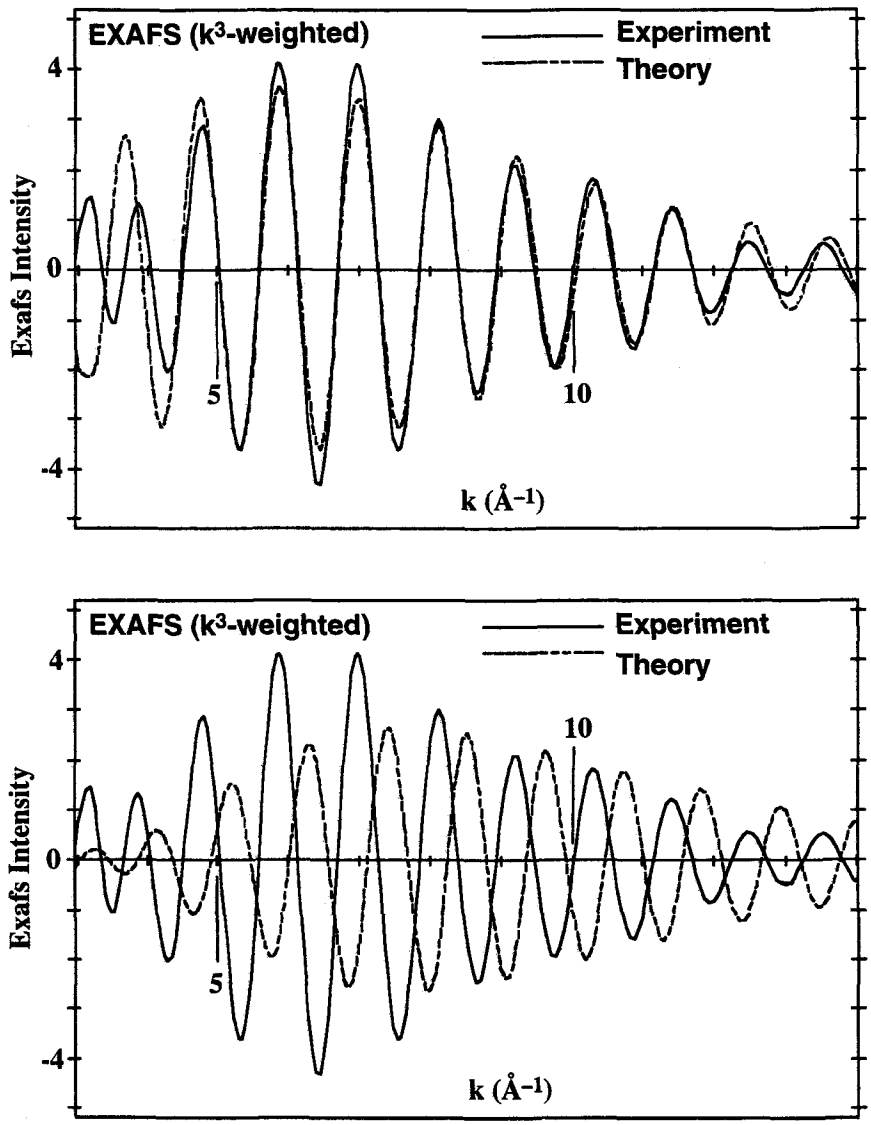

Figure 6. Comparison of model XAS fine structure for a single shell of 6 atoms of Mg (top panel) or 2 atoms of Fe (bottom panel) at 3.12 Å to the experimental data of Figure 5 (Fe:Mg 1:4 pyroaurite) Fourier-filtered from 2.2 to 4 Å (isolated second shell contibution). In both cases the appropriate model parameters from Table 3 have been retained (apart from number and type of atom). It is clear that the experimental second shell EXAFS is in phase with the backscattering from a hypothetical Mg shell at 3.12 Å, but out of phase with an Fe one; thus the presence of Fe in the second shell around the Fe absorber would be easily detected.

order in the lattice, resulting in some destructive interference of the scattered X-rays from successive unit cells. This is an interesting result in view of the fact that in nature pyroaurites usually seems to occur in the 1:3 Fe:Mg form (Allmann 1968; Drits et al. 1987) and that there is some evidence that hydrothermal synthesis at elevated temperature and pressure results in the formation of 1:3 Fe:Mg pyroaurite from 1:2 mother liquor (Vucelic et al. 1995). The Debye–Waller factor described above gives some support to the idea that, at high concentrations, the trivalent cations result in greater distortion of the lattice, resulting in more static disorder, and this would fit well with the 1:2 Fe:Mg form being destabilized.

A final point of interest is the absence of strong features beyond 3.5 Å in the PRDFs of the pyroaurites, notably the lack of a large second cation shell at 5.40 Å. There is a triplet of peaks present above the noise level in all 3 PRDFs between 4.5 Å and 6.5 Å; however, due to the low intensity of these features and the complexity of the possible single and multiple scattering paths responsible for them, it has proved impossible to obtain additional useful structural information from these features. Although one expects a rapid fall-

off in backscattering with distance, some EXAFS would still be expected out to at least 6 Å, particularly in the case of a shell consisting largely of relatively strong backscatterers (Fe). The absence of such a feature suggests a considerable degree of static disorder in the lattice, resulting in a distribution of distances for the longer coordination spheres and so a smearing out of the EXAFS. Such an effect could be caused, for example, by the presence of significant numbers of random cation substitutions within the LDH sheets. To test this idea, spectra were recorded for the same pyroaurites at liquid nitrogen temperatures. This should radically reduce the thermal agitation of the lattice and, in the absence of static disorder, allow resolution of shells at larger distances. In fact, the liquid nitrogen temperature spectra were effectively indistinguishable from those taken at room temperature, confirming the presence of substantial amounts of static disorder within the lattice.

CONCLUSION

We have demonstrated in this paper that, although there is no long-range Fe(III) cation ordering in pyroaurites, there is a high degree of local order, taking the form of Fe cations never (within the detection limits of XAS) neighboring each other. These 2 results can be consistent only if there are reasonably frequent defects to the ideal cation pattern, probably roughly every fifth to tenth cation in any direction. This would result in coherent superlattice domains never exceeding a few tens of angstroms, and so remaining X-ray invisible, while only a few percent of sites would be affected and the average environment around absorbing Fe atoms would thus remain effectively unchanged. Two types of defect can be envisaged. There may be cation vacancies or a Mg cation may substitute into a site that would ideally be occupied by an Fe cation. Both types of defect would disrupt the long-range order of the cation superlattice, while leaving the remaining coherent scattering from the brucite-like layers unaffected.

It seems almost certain that these results can be generalized both to LDHs with other types of divalent and trivalent cations (such as Mg/Al, Mg/Ni and Ni/Al) and to situations where different interlayer anions are present. In all cases synthesis proceeds via the same route, an amorphous hydroxide precipitate initially forming, followed by a long period of digestion as the layers order and cation substitutions occur and the layers are brought together by interlayer anions. The only system in which this pattern is varied is the case of Li/Al LDHs. In this case, the Li substitutes into the naturally occurring vacancies in the gibbsite-like $Al(OH)_3$ lattice. Thus, swapping of divalent for trivalent cations is not necessary in the ordering process, merely the diffusion of the Li ions into the preexisting vacancies of the $Al(OH)_3$ layers. Clearly the ordering of vacancies during digestion is expected to be a more facile process than interchange of cations between sites. Indeed, in the case of Li/Al LDHs, strong diffraction features from the Li superlattice (with a lattice parameter of $\sqrt{3}a$) are always observed.

It is interesting that although diffraction features from cation ordering in M(II)/M(III) LDHs have never been observed, reflections resulting from the ordering of anions within the interlayer region have been reported, both in the case of LDH benzoate and sulphate (Bookin et al. 1993; Vucelic et al. 1995). Thus there must be a mismatch between the positions of positive charges in the brucite-like layers and the anions balancing those charges. The anion positions must principally be determined by geometric considerations and the optimization of hydrogen bonding rather than ensuring maximum coulombic attractions to the positively charged sheets. With this in mind, it would be interesting to compare sulphate or benzoate (which both show long-range anion order with $\sqrt{3}a$ lattice parameter in LDHs) stability as the anion in Li/Al LDH (with long-range cation order) to their stability in an M(II)/M(III) LDH (lacking long-range cation order). There have been reports (Sissoko et al. 1985; Borja and Dutta 1992) that Li/Al and Mg/Al LDHs show different ion exchange properties and the matching of cation and anion ordering may be part of the explanation for this phenomenon.

ACKNOWLEDGMENTS

The authors would like to thank P. Parent for assistance with the XAS experiments at LURE and D. Vucelic for provision of powder XRD facilities at the Institute for General and Physical Chemistry, Belgrade. MVV holds a Commonwealth Trust Fellowship and an Overseas Research Fellowship. GDM carried out this work with the assistance of an European Union Human Capital and Mobility Fellowship and a King's College (Cambridge) Research Fellowship.

REFERENCES

Allmann R. 1968. The structure of pyroaurite. Acta Crystallogr B24:972–977.

Allmann R. 1970. Doppelschichtstukturen mit brucitähnlichen Schichtionen $[Me(II)_{1-x}\ Me(III)_x\ (OH)_2]^{x+}$. Chimia 24: 99–108.

Bookin AS, Cherkashin VI, Drits VA. 1993. Polytype diversity of the hydrotalcite-like minerals. II. Determination of the polytypes of experimentally studied varieties. Clays Clay Miner 41(5):558–564.

Bookin AS, Drits VA. 1993. Polytype diversity of the hydrotalcite-like minerals. I. Possible polytypes and their diffraction features. Clays Clay Miner 41(5):551–557.

Borja M, Dutta PK. 1992. Fatty acids in layered metal hydroxides; membrane-like structure and dynamics. J Phys Chem 96:5434–5444.

Brindley GW, Kikkawa S. 1979. A crystal-chemical study of Mg, Al and Ni, Al hydroxy-perchlorates and hydroxy-carbonates. Am Mineral 64:836–843.

Chibwe K, Jones W. 1989. Intercalation of organic and inorganic anions into layered double hydroxides. J Chem Soc, Chem Commun 14:926–927.

De Waal SA, Viljoen EA. 1971. Nickel minerals from Barberton, South Africa. IV. Reevesite, a member of the hydrotalcite group. Am Mineral 56:1077–1081.

Drezdon MA. 1988. Synthesis of isopolymetalate-pillared hydrotalcite via organic-anion-pillared precursors. Inorg Chem 27:4628–4632.

Drits VA, Sokolova TN, Sokolova GV, Cherkashin VI. 1987. New members of the hydrotalcite-manasseite group. Clays Clay Miner 35(6):401–417.

Dutta PK, Puri M. 1988. Anion exchange in lithium aluminium hydroxides. J Phys Chem 93:376–381.

Frondel C. 1941. Constitution and polymorphism of the pyroaurite and sjögrenite groups. J Mineral Soc Am 26(5): 295–315.

Gastuche MC, Brown G, Mortland MM. 1967. Mixed magnesium–aluminium hydroxides. Clay Miner 7:177–192.

Hansen HCB, Taylor RM. 1990. Formation of synthetic analogues of double metal-hydroxy carbonate minerals under controlled pH conditions. Clay Miner 25:161–179.

Hansen HCB, Taylor RM. 1991. The use of glycerol intercalates in the exchange of CO_3^{2-} with SO_4^{2-}, NO_3^- or Cl^- in pyroaurite-type compounds. Clay Miner 26:311–327.

Jones W. 1991. Utilising clays and layered solids. Univ of Wales Rev, Sci and Technol 8:45–52.

Kuma K, Paplawsky W, Gedulin B, Arrhenius G. 1989. Mixed valence hydroxides as bioorganic host minerals. Origins of Life and Evolution of the Biosphere 19:573–602.

Miyata S. 1975. The synthesis of hydrotalcite-like compounds and their structure and physico-chemical properties. Clays Clay Miner 23:369–375.

Miyata S. 1980. Physico-chemical properties of synthetic hydrotalcites in relation to composition. Clays Clay Miner 28: 50–56.

Pausch I, Lohse H-H, Schürmann K, Allmann R. 1986. Synthesis of disordered and Al-rich hydrotalcite-like compounds. Clays Clay Miner 34(5):507–510.

Reichle WT. 1985. Catalytic reactions by thermally activated, synthetic, anionic clay minerals. J Catal 94:547–557.

Serna CJ, Rendon JL, Iglesias JE. 1982. Crystal-chemical study of layered $[Al_2Li(OH)_6]^+ X^- \cdot nH_2O$. Clays Clay Miner 30(3):180–184.

Sissoko I, Iyagba E.T, Sahai R, Biloen P. 1985. Anion intercalation and exchange in $Al(OH)_3$-derived compounds. J Solid State Chem 60:283–288.

Taylor HFW. 1969. Segregation and cation ordering in sjögrenite and pyroaurite. Mineral Mag 37(287):338–342.

Taylor HFW. 1973. Crystal structures of some double hydroxide minerals. Mineral Mag 39(304):377–389.

Ulibarri MA, Hernandez MJ, Corneto J. 1987. Changes in textural properties derived from the thermal decomposition of synthetic pyroaurite. Thermochim Acta 63:154.

Vucelic M, Moggridge GD, Jones W. 1995. The thermal properties of terephthalate and benzoate intercalated LDH. J Phys Chem 99(20):8328–8337.

(Received 13 September 1996; accepted 27 January 1997; Ms. 2796)